(2)

COLLEGE PARK CAMPUS

Quality Assessment of the A-posteriori Error Estimation in Finite Elements

by

Ivo Babuška
Lothar Plank
and
Rodolfo Rodríguez

Technical Note BN-1127

August 1991

INSTITUTE FOR PHYSICAL SCIENCE AND TECHNOLOGY

SECURITY CLASSIFICATION OF THIS PAGE (When Data Entered)

REPORT DOCUMENTATION PAGE		READ INSTRUCTIONS BEFORE COMPLETING FORM
1. REPORT NUMBER Technical Note BN-1127	2. GOVT ACCESSION NO.	3. RECIPIENT'S CATALOG NUMBER
4. TITLE (and Subtitle) Quality Assessment of the A-posteriori Error Estimation in Finite Elements		5. TYPE OF REPORT & PERIOD COVERED Final Life of the Contract 6. PERFORMING ORG. REPORT NUMBER
7. AUTHOR(s) Ivo Babuska[1] - Lothar Plank[2] and Rodolfo Rodriguez[3]		8. CONTRACT OR GRANT NUMBER(s) [1]ONR N00014-90-J-1030 [2]NSF CCR-88-20279 [3]NSF CCR-88-20279
9. PERFORMING ORGANIZATION NAME AND ADDRESS Institute for Physical Science and Technology University of Maryland College Park, MD 20742-2431		10. PROGRAM ELEMENT, PROJECT, TASK AREA & WORK UNIT NUMBERS
11. CONTROLLING OFFICE NAME AND ADDRESS Department of the Navy Office of Naval Research Arlington, VA 22217		12. REPORT DATE August 1991 13. NUMBER OF PAGES 25
14. MONITORING AGENCY NAME & ADDRESS(if different from Controlling Office)		15. SECURITY CLASS. (of this report) 15a. DECLASSIFICATION/DOWNGRADING SCHEDULE

16. DISTRIBUTION STATEMENT (of this Report)

Approved for public release: distribution unlimited

17. DISTRIBUTION STATEMENT (of the abstract entered in Block 20, if different from Report)

18. SUPPLEMENTARY NOTES

19. KEY WORDS (Continue on reverse side if necessary and identify by block number)

20. ABSTRACT (Continue on reverse side if necessary and identify by block number)

The paper addresses results of numerical experimentation with an a-posteriori error estimator which was theoretically analyzed in [1]. The paper concentrates on the problems of the selection of benchmarks which is directed to a numerical verification of basic theoretical features of the estimator.

DD FORM 1 JAN 73 1473 EDITION OF 1 NOV 65 IS OBSOLETE
S/N 0102-LF-014-6601

SECURITY CLASSIFICATION OF THIS PAGE (When Data Entered)

Quality Assessment of the A-posteriori Error Estimation in Finite Elements

Ivo Babuška [1] Lothar Plank [2] Rodolfo Rodríguez [3]

August 1991

[1]Institute for Physical Science and Technology and Department of Mathematics, University of Maryland, College Park, MD 20740. The work of this author was partially supported by the ONR under grant N00014-90-J-1030.

[2]Institute for Physical Science and Technology and Department of Mathematics, University of Maryland, College Park, MD 20740. The work of this author was partially supported by the NSF under grant CCR-88-20279.

[3]Institute for Physical Science and Technology and Department of Mathematics, University of Maryland, College Park, MD 20740 and Departamento de Matemática, Facultad de Ciencias Exactas, Universidad Nacional de La Plata, C.C. 172, 1900 - La Plata, Argentina. The work of this author was partially supported by the NSF under grant CCR-88-20279.

Abstract

The paper addresses results of numerical experimentation with an a-posteriori error estimator which was theoretically analyzed in [1]. The paper concentrates on the problems of the selection of benchmarks which is directed to a numerical verification of basic theoretical features of the estimator.

1 Introduction

During recent years much interest has been focused on the design of a-posteriori error estimates in the finite element method, their experimental verification and their use for adaptive procedures. We refer for example to [1-24] and further citations there.

The a-posteriori error estimators are often derived by purely heuristic reasoning and without mathematical analysis. If a mathematical analysis is made it adresses most often only asymptotic properties and special meshes. Usually the estimators are numerically analyzed (verified) on a set of examples (benchmarks) which are selected at best by heuristic reasoning. Often these benchmark computations are used for the design of a correction factor which is used to improve the quality of the estimators for this set of benchmarks.

This pragmatic approach to test and compare the estimators by benchmark computations has serious shortcomings. The quality of an estimator is usually very sensitive to the structure of the solution and the meshes used. The performance of an estimator can be very different. It may depend on whether the meshes are nearly translation invariant or general, or whether the meshes are general or such that the error indicators are nearly equal on all elements (i.e. the meshes are equilibrated), or whether the solution is smooth, has point singularities or is generally unsmooth, etc. Some of these aspects are adressed in [5]. Hence the benchmark computations could motivate misleading conclusions. Each benchmark computation should be a representative of a more or less precisely defined class of computational problems and the conclusions used for this class of problems.

In this paper we will address various aspects of the relation between theoretical understanding of an estimator and the benchmark selection. We will adress a certain estimator which is used in practice, and discuss its properties. We do not intend to compare it with any other error estimator.

2 The Model Problem

Let $\Omega \in \mathbf{R}^2$ be a bounded polygonal domain and let Γ be its boundary. Assume further that $\overline{\Omega} = \cup_{i=1}^m \overline{\Omega_i}$, where Ω_i is a polygonal domain (with boundary $\partial\Omega_i$) and that $\Omega_i \cap \Omega_j = \emptyset$ for $i \neq j$. We will be interested in solving the following problem:

$$-\operatorname{div}(a\nabla u) = f \ \text{ in } \ \Omega, \quad u = 0 \text{ on } \Gamma_D, \quad a\frac{\partial u}{\partial \mathbf{n}} = g \text{ on } \Gamma_N, \ \ \Gamma_D \cup \Gamma_N = \Gamma, \tag{2.1}$$

where $\mathbf{n}$ is the outward normal to Ω. We assume that $f \in H^1(\Omega)$, $g \in H^1(\Gamma_D)$, $a \geq a_0 \geq 0$ is constant on $\Omega_i, i = 1, \ldots, m$, We will assume that either meas$(\Gamma_D) \neq 0$ or, if $\Gamma_D = \emptyset$, $\int_\Omega f dxdy + \int_\Gamma g ds = 0$ and $u(A) = 0$, $A \in \overline{\Omega}$. (Because of the assumptions about f and g, $u \in H^\alpha(\Omega), \alpha > 1$, and so $u(A) = 0$ makes sense.)

We will consider the weak solution of (2.1). To this end we denote by $H^k(\Omega)$ the usual Sobolev space and let

$$H_0^1 = \left\{u \in H^1(\Omega), u = 0 \text{ on } \Gamma_D\right\}$$

Further we let

$$B(u,v) = \int_\Omega a(\frac{\partial u}{\partial x}\frac{\partial v}{\partial x} + \frac{\partial u}{\partial y}\frac{\partial v}{\partial y})dxdy \tag{2.2}$$

be the bilinear form defined on $H_0^1(\Omega) \times H_0^1(\Omega)$ and

$$F(v) = \int_\Omega f v dx dy + \int_{\Gamma_N} g v ds. \tag{2.3}$$

be a linear functional on $H_0^1(\Omega)$. Then the weak solution u of (2.1) in H_0^1 exists, is unique and

$$B(u,v) = F(v) \quad \forall v \in H_0^1. \tag{2.4}$$

If $\Gamma_D = \emptyset$, we consider $H^1(\Omega)$ instead of $H_0^1(\Omega)$ and assume $u(A) = 0$, which is well-defined, as we have in fact higher regularity for u.

Let us consider a family $\mathcal{M}$ of triangular meshes M on Ω satisfying a uniform minimal angle condition. We denote by $\mathcal{T}$ the closed triangles of the mesh M, $\bigcup \mathcal{T} = \overline{\Omega}$. We will assume that if $\mathcal{T} \in M$ then interior$(\mathcal{T}) \subset \Omega_l$ for some l, i.e. $\mathcal{T}$ lies in a domain where a is a constant. To every mesh M we associate a parameter $t(M) \geq 0$, for example $t(M) = N^{-1}$ where N is the number of the nodes that do not belong to Γ_D or $t(M) = h$ where $h = \max(d(\mathcal{T}))$ and $d(\mathcal{T})$ denotes the diameter of $\mathcal{T}_j$. We will always assume that $h = \max(d(\mathcal{T}_j)) \to 0$ as $t(M) \to 0$.

Further let $S(M)$ be the set of all continuous functions on Ω whose restriction on a $\mathcal{T} \in M$ is a linear function. Obviously $S(M) \subset H^1(\Omega)$. Let $S_0(M) = H_0^1(\Omega) \cap S(M)$ and $S_A(M) = \{u \in S(M),\ u(A) = 0\}$. Then the finite element solution $u_S \in S_0(M)$ satisfies

$$B(u_S, v) = B(u, v) \quad \forall v \in S_0(M) \tag{2.5}$$

where u is the exact solution of (2.1). If $\Gamma_D = \emptyset$, we replace $S_0(M)$ by $S_A(M)$. We will consider a family of finite element solutions u_S associated to $\mathcal{M}$ and assume that $\|u - u_{S(M)}\|_E = B(u - u_{S(M)}, u - u_{S(M)})^{\frac{1}{2}} \to 0$ as $t(M) \to 0$. By (2.5) we associate to any solution u its finite element solution $u_S = u_S(M, u)$ and an error estimator $\mathcal{E}(u, M)$ that will be defined in the next section. In fact $\mathcal{E}$ depends on u_S and M but because of (2.5) we write $\mathcal{E}(u, M)$. This estimator approximates the energy norm of the error, i.e. $\mathcal{E}(u, M) \approx \|e\|_E = (B(e, e))^{1/2}$, where $e = u - u_S$.

3 The Error Estimator

Let $M \in \mathcal{M}$, $\mathcal{T}_i, \mathcal{T}_l \in M$ be two triangles with common side $\gamma_{l,i}$ as shown in figure (3.1). By $\mathbf{n}_{l,i}$ we denote the outer normal from $\mathcal{T}_l$ to $\mathcal{T}_i$; we will also write $\mathcal{T}_l = \mathcal{T}_{\text{in}}$ and $\mathcal{T}_i = \mathcal{T}_{\text{out}}$, as $\mathcal{T}_{\text{in}}$ is the triangle for which the normal $\mathbf{n}_{l,i}$ is the outward one.

Let us now define for every side $\gamma_{l,i}$

$$\left[\!\left[a \frac{\partial u_S}{\partial \mathbf{n}_{l,i}} \right]\!\right](x) = (a \nabla u_S)\big|_{\mathcal{T}_{\text{out}}} \cdot \mathbf{n}_{l,i} - (a \nabla u_S)\big|_{\mathcal{T}_{\text{in}}} \cdot \mathbf{n}_{l,i} \tag{3.1}$$

the jump of $a \frac{\partial u_S}{\partial \mathbf{n}_{l,i}}$ across the side $\gamma_{l,i}$. This value is independent of the choice of $\mathbf{n}_{l,i}$, i.e. $\left[\!\left[a \frac{\partial u_S}{\partial \mathbf{n}_{l,i}} \right]\!\right](x) = \left[\!\left[a \frac{\partial u_S}{\partial \mathbf{n}_{i,l}} \right]\!\right](x)$ and so we will write $\left[\!\left[a \frac{\partial u_S}{\partial \mathbf{n}} \right]\!\right](x)$.

For each triangle $\mathcal{T} \in M$ let

$$R_{\mathcal{T}} = -\left[\operatorname{div}(a \nabla u)\,|_{\mathcal{T}} + \operatorname{div}(a \nabla u_S)\,|_{\mathcal{T}}\right] + f\,|_{\mathcal{T}}\,. \tag{3.2}$$

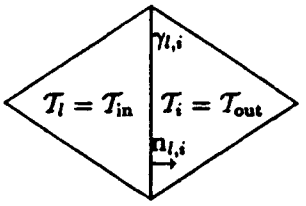

Figure 3.1: Scheme of neighbouring elements

We may write for any $v \in H_0^1$ the residual equation

$$B(e,v) = \sum_{\mathcal{T}\in M} \int_{\mathcal{T}} R_{\mathcal{T}} v dx dy + \int_{\Gamma_N} (g - a\frac{\partial u_S}{\partial \mathbf{n}}) v ds + \sum_{\gamma \in G} \int_{\gamma} \left[\!\left[a \frac{\partial u_S}{\partial \mathbf{n}} \right]\!\right] v ds \tag{3.3}$$

where G stands for the set of all interior edges of M and $\mathbf{n}$ for the outward normal to Ω. (If $\Gamma_D = \emptyset$ the equation (3.3) is the same, but $v \in H^1(\Omega)$.)

For any $\mathcal{T} \in M$ we define

$$\Pi_{\mathcal{T}} = \frac{1}{|\mathcal{T}|} \int_{\mathcal{T}} R_{\mathcal{T}} dx dy \tag{3.4}$$

where $|\mathcal{T}|$ is the area of $\mathcal{T}$. ($\Pi_{\mathcal{T}}$ is the $L^2(\mathcal{T})$ projection of the interior residual onto the set of constants.) Further for each $\gamma \in \Gamma_N$, where γ is a side of a triangle $\mathcal{T}$, we define

$$\Pi_{\gamma} = \frac{1}{|\gamma|} \int_{\gamma} (g - \frac{\partial u_S}{\partial \mathbf{n}}) ds \tag{3.5}$$

where $|\gamma|$ is the length of γ. (Π_{γ} is the $L^2(\gamma)$ projection of the boundary residual onto the set of constants.)

For each edge γ of the mesh let

$$J_{\gamma} = \begin{cases} \left[\!\left[a\frac{\partial u_S}{\partial \mathbf{n}} \right]\!\right] & \text{if } \gamma \in G \\ 2\Pi_{\gamma} & \text{if } \gamma \subset \Gamma_N \\ 0 & \text{if } \gamma \subset \Gamma_D \end{cases} \tag{3.6}$$

and for each triangle $\mathcal{T} \in M$ we define the error indicator $\eta_{\mathcal{T}}$:

$$\eta_{\mathcal{T}} := \left[|\mathcal{T}| \int_{\mathcal{T}} \frac{\Pi_{\mathcal{T}}^2}{a} dx dy + \frac{1}{2} \sum_{\gamma \in \partial \mathcal{T}} |\gamma| \int_{\gamma} \frac{J_{\gamma}^2}{a\,|_{\mathcal{T}}} ds \right]^{\frac{1}{2}} \tag{3.7}$$

which approximates the energy error on $\mathcal{T}$. Further we define the error estimator

$$\mathcal{E}(u,M) := \left(\sum_{\mathcal{T}\in M} \eta_{\mathcal{T}}^2 \right)^{\frac{1}{2}} \kappa \tag{3.8}$$

where κ is a suitable constant which will be defined later. It is convenient to write

$$\mathcal{E}^*(u,M) := \left(\sum_{\mathcal{T}\in M} \eta_{\mathcal{T}}^2 \right)^{\frac{1}{2}} \tag{3.9}$$

for the choice $\kappa = 1$. Let us note that the error indicator is meaningful for more general f and g than we have assumed. Nevertheless our generality is sufficient for practical purposes. Obviously the set of problems we are discussing is precisely described.

4 The Quality of the Error Estimator

In Section 3 we defined the error estimator $\mathcal{E}(u, M)$ which approximates $\|e\|_E$. In the following we will discuss the relation between $\mathcal{E}(u, M)$ and $\|e\|_E$, especially the effectivity index of the estimator

$$\xi = \frac{\mathcal{E}(u, M)}{\|e\|_E}.$$

Before addressing this problem we introduce some notation which we will need in the following. Let $S^p(M)$ be the space of all continuous functions on Ω whose restriction on $T \in M$ is a polynomial of degree p. Let $S_0^p(M) = S^p \cap H_0^1(\Omega)$ and $u_S^p \in S_0^p(M)$ be the finite element solution of problem (2.1), i.e.

$$B(u_S^p, v) = B(u, v) \quad \forall v \in S_0^p(M)$$

(If $\Gamma_D = \emptyset$, we use $S_A^p(M)$ instead of $S_0^p(M)$.) Obviously u_S^p is the p-version solution of problem (2.1). For more about the $h-p$-version we refer to [6]. We have for any $k > 1$:

$$\|u_S^p - u\|_E \leq Cp^{-(k-1)}\|u\|_{H^k} h^{\min\{p, k-1\}} \tag{4.1}$$

with C dependent on k, but not on p and h.

Remark: Although in (4.1) the maximal element side is used, an analogous element by element estimate holds.

Now we are able to state the basic theorems about $\mathcal{E}^*(u, M)$. (See [1] for the detailed proof and Section 5 for an outline of the main ideas.)

Theorem 4.1 *For any integer p there is a constant K_2^p depending only on the minimal angle α_T of the triangles used and on p, such that*

$$\|e\|_E \leq K_2^p \mathcal{E}^*(u, M) + \|u - u_S^p\|_E + O(h^{\frac{3}{2}}) \tag{4.2}$$

and the constant K_2^p grows logarithmically with p.

Theorem 4.2 *There is a constant $K_1 > 0$, depending only on α_T and on the jumps of a, such that*

$$\mathcal{E}^*(u, M) \leq K_1 \|e\|_E + O(h^{\frac{3}{2}}). \tag{4.3}$$

The constants K_1 and K_2^p are computable. We have

$$K_2^p = \max_{T \in M} C_T^p \tag{4.4}$$

and

$$K_1 = (\max_{T \in M} C_T')Q_a, \tag{4.5}$$

where

$$Q_a = \max_{T \cap T' \neq \emptyset} \left(\frac{a|_T}{a|_{T'}}\right). \tag{4.6}$$

For $2 \leq p \leq 8$ we have the estimates

$$.548 \log^{\frac{1}{2}} p \sin^{-\frac{1}{2}}\left(\frac{\alpha_T}{2}\right) \leq C_T^p \leq .813 \log^{\frac{1}{2}} p \sin^{-\frac{1}{2}}\left(\frac{\alpha_T}{2}\right) \tag{4.7}$$

α	C'_T	C^p_T			
		$p=2$	$p=4$	$p=6$	$p=8$
7.5	.051	2.390	3.306	3.660	3.988
15.0	.072	1.682	2.341	2.609	2.839
22.5	.087	1.363	1.918	2.156	2.343
30.0	.099	1.169	1.670	1.895	2.058
37.5	.108	1.035	1.508	1.727	1.876
45.0	.115	.939	1.400	1.615	1.757
52.5	.119	.875	1.334	1.547	1.684
60.0	.121	.850	1.309	1.522	1.657

Table 4.1: Constants C^p_T and C'_T for various angles α_T

and

$$3.45 \sin^{-\frac{1}{2}}(\frac{\alpha_T}{2}) \leq C'_T \leq 5.85 \sin^{-\frac{1}{2}}(\frac{\alpha_T}{2}) \tag{4.8}$$

where α_T is the minimal angle of T. In Table 4.1 we give the values of C^p_T and C'_T.

Let us note that for h small only very few elements have a side on the interface $\partial\Omega$; we can in fact use $Q_a = 1$.

Remark: We have dealt only with the Laplace equation. In this case we use the minimal angle α_T of the triangle. For a general differential equation we have to replace it by α'_T which is the minimal angle of the triangle after a local transformation of the general equation to Laplace's equation (this is always possible).

The term $O(h^{\frac{1}{2}})$ in (4.2) and (4.3) depends only on $\|f\|_{H^1(\Omega)}$ and $\|g\|_{H^1(\Gamma)}$, but not on u. For any u the term $\|u - u^p_S\|_E$ can be made arbitrarily small by (4.1) using sufficiently large p. We note that the smoothness of u is governed by the smoothness of f and g, transition of boundary conditions and smoothness of Γ. It is unessential that the estimates (4.2) and (4.3) have an asymptotic character. For example if f = const on every T and g = const on every triangle side of Γ_N, the term $O(h^{\frac{1}{2}})$ disappears. Hence as $t(M) \to 0$, the term $O(h^{\frac{1}{2}})$ is negligible in general.

Theorems 4.1 and 4.2 indicate that the error estimator $\mathcal{E}^*(u, M)$ can be either smaller or bigger than the true error. Further the error estimator loses accuracy when $\alpha_T \to 0$ and for unsmooth u the reliability of the estimator decreases because a higher p is needed in the estimator.

The coefficient κ, which scales the error estimator ($\mathcal{E}(u, M) = \kappa\mathcal{E}^*(u, M)$), can be calculated in different ways. We can use the geometrical average of the bounds in (4.4), (4.5). Another possibility is to choose κ such that the error estimator is asymptotically exact for uniform meshes of equilateral triangles and $f = 0$. In this case we get $\kappa = (\sqrt{8\sqrt{3}})^{-1} \approx 0.26864$ which will be used for all examples.

Theorems 4.1 and 4.2 indicate the expected theoretical properties of the estimator well. The structure of Theorems 4.1 and 4.2 clearly suggests the set of benchmark experiments that should be performed.

5 The Outline of the Proof of Theorems 4.1 and 4.2

For simplicity assume that f and g are constant on each $\mathcal{T}$ resp $l \in \Gamma_N$. (The general case is discussed in [1].) With $e_p := u_S^p - u_S \in S_0^p$, we have

$$\|e\|_E \le \|e_p\|_E + \|u - u_S^p\|_E \tag{5.1}$$

and

$$\|e_p\|_E^2 = B(e_p, e_p) = B(u_S^p - u, e_p) + B(u - u_S, e_p) = B(e, e_p) \tag{5.2}$$

For any continuous function v let v^I denote the linear interpolant of v on $\mathcal{T}$. Using (3.3), we have:

$$\begin{aligned}
\|e_p\|_E^2 = B(e, e_p) &= \sum_{T \in M} \left[\int_T \Pi_T (e_p - e_p^I) dx dy + \frac{1}{2} \sum_{l \subset \partial T} \int J_l (e_p - e_p^I) ds \right] \\
&\le \sum_{T \in M} \eta_T \left\{ \left[\frac{\sqrt{a|_T}}{|T|} \int_T (e_p - e_p^I) dx dy \right]^2 + \frac{1}{2} \sum_{l \subset \partial T} \left[\frac{\sqrt{a|_T}}{|l|} \int_l (e_p - e_p^I) ds \right]^2 \right\}^{1/2} \\
&\le \sum_{T \in M} \eta_T C_T^p \|e_p\|_{E,T}
\end{aligned}$$

where

$$C_T^p = \sup_{v \in P_p \setminus P_0} \left(\frac{\frac{1}{|T|} |\int_T (v - v^I) dx dy|^2 + \frac{1}{2} \sum_{l \subset \partial T} |\frac{1}{|l|} \int_l (v - v^I) ds|^2}{\int_T |\nabla v|^2 dx dy} \right)^{1/2}$$

Here, P_p and P_0 denote the spaces of all polynomials of degree p or 0 on $\mathcal{T}$, respectively.

Hence

$$\|e_p\|_E \le K_2^p \mathcal{E}^*(u, M)$$

with

$$K_2^p = \sup_{T \in M} C_T^p.$$

Using (5.1) we get (4.2) without the term $O(h^{3/2})$. This is related to the simplification assumption about f and g made in this section.

Let us now address inequality (4.3). For any triangle $\mathcal{T}$ as shown in Fig. 5.1, let φ_0 be the cubic bubble function vanishing on $\partial \mathcal{T}$ with $\varphi_0(Q_0) = 1$, where Q_0 is the barycenter of $\mathcal{T}$. Let

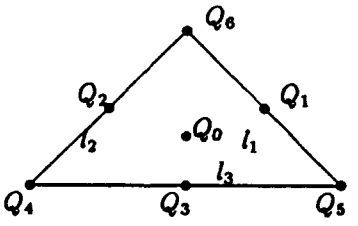

Figure 5.1: Notation for triangular elements

further $\mathcal{P}_2^0(\mathcal{T})$ be the space of quadratic functions vanishing at the vertices of $\mathcal{T}$ and let $\{\varphi_l\}_{l=1}^3$

be the canonical basis of this space (i.e. $\varphi_i(Q_j) = \delta_{ij}, i = 1,2,3, j = 1,\ldots,6$) and let V_T be the space spanned by $\{\varphi_l\}_{l=0}^3$. Set $\omega_T = \sum_{l=0}^3 \omega_i\varphi_i \in V_T$ with coefficients $\omega_0,\omega_1,\omega_2,\omega_3$ chosen such that

$$\int_T \Pi_T\omega_T dxdy = |T| \int_T \frac{\Pi_T^2}{a} dxdy \tag{5.3}$$

$$\int_{l_i} J_{l_i}\omega_T ds = |l_i| \int_{l_i} \frac{J_{l_i}^2}{[a]_{l_i}} ds, \quad i = 1,2,3 \tag{5.4}$$

where $[a]_{l_i}$ is the average of a over the triangles sharing the edge l_i, i.e.

$$[a]_{l_i} = \begin{cases} \frac{1}{2}(a\,|_{T_{\text{in}}} + a\,|_{T_{\text{out}}}) & \text{if } l_i = \partial T_{\text{in}} \cap \partial T_{\text{out}} \\ a\,|_T & \text{if } l_i \subset \partial T \cap \Gamma \end{cases} \tag{5.5}$$

The coefficients $\omega_0,\ldots,\omega_3$ satisfying (5.3) and (5.4) are

$$\begin{aligned} \omega_i &= \frac{3|l_i|}{2[a]_{l_i}} \\ \omega_0 &= \frac{20}{9}\left(\frac{|T|\mathcal{R}_T}{a\,|_T} - \frac{1}{2}\sum_{i=1}^3 \frac{|l_i|}{[a]_{l_i}} J_{l_i}\right) \end{aligned}$$

Since for any interior edge l he values ω_{T_l} are the same on both triangles T sharing the edge, the function ω composed from ω_T on every triangle is continuous and hence $\omega \in H_0^1(\Omega)$. Using (5.1), (5.2) we get:

$$\begin{aligned} (\mathcal{E}^*(u,M))^2 &= \sum_{T\in M} \eta_T^2 \\ &= \sum_{T\in M}\left[|T| \int_T \frac{\Pi_T^2}{a} dxdy + \frac{1}{2}\sum_{l\in\partial T} |l| \int_l \frac{J_l^2}{a\,|_T} ds\right] \\ &= \sum_{T\in M}\left[\int_T \Pi_T\omega_T dxdy + \frac{1}{2}\sum_{l\in\partial T} \frac{[a]_l}{a\,|_T} \int_l J_l\omega_T ds\right] \\ &\le C_a \sum_{T\in M}\left[\int_T \Pi_T\omega_T dxdy + \frac{1}{2}\sum_{l\in\partial T} \int_l J_l\omega_T ds\right] \end{aligned}$$

where

$$C_a = \max_{l\in\partial T, T\in M} \frac{[a]_l}{a\,|_T}.$$

Since $\omega \in H_0^1$ we get from (3.3)

$$(\mathcal{E}^*(u,M))^2 \le C_a B(e,\omega) \le C_a \|e\|_E \|\omega\|_E. \tag{5.6}$$

Now let for $\mathbf{r} = \{r_i\}_{i=0}^3$

$$C_T'^2 = \sup_{\|\mathbf{r}\|\neq 0} \frac{\int_T \|\nabla v_\mathbf{r}\|^2 dxdy}{r_0^2 + \frac{1}{2}\sum_{i=1}^3 r_i^2}$$

where $v_\mathbf{r} \in V_T$ is the function satisfying $\int_T v_\mathbf{r} dxdy = |T|r_0$, $\int_{l_i} v_\mathbf{r} ds = |l_i|r_i$, $i = 1,2,3$. Therefore ω_T is the function $v_\mathbf{r}$ corresponding to

$$\begin{aligned} r_0 &= \frac{|T|\Pi_T}{a\,|_T} \\ r_i &= \frac{|l_i|J_{l_i}}{[a]_{l_i}}, \quad i = 1,2,3 \end{aligned}$$

and so

$$\begin{aligned}
\|\omega_T\|^2_{E,T} &= a|_T \int_T \|\nabla v_x\|^2 dx dy \\
&\leq C'^2_T a|_T \left(\frac{|T|^2 \Pi^2_T}{a|_T{}^2} + \frac{1}{2} \sum_{i=1}^{3} \frac{|l_i|^2 J^2_{l_i}}{[a]^2_{l_i}} \right) \\
&= C'^2_T \left(\frac{|T|^2 \Pi^2_T}{a|_T} + \frac{1}{2} \sum_{i=1}^{3} \left(\frac{a|_T}{[a]_{l_i}} \right)^2 \frac{|l_i|^2 J^2_{l_i}}{a|_T} \right) \\
&\leq C'^2_T C'^2_a \eta^2_T,
\end{aligned}$$

where

$$C'_a = \max_{l \subset \partial T, T \in M} \frac{a|_T}{[a]_l}.$$

Hence

$$\|\omega\|_E \leq (\max_{T \in M} C'_T) C'_a \mathcal{E}^*(u, M)$$

and so, using 5.6, we obtain

$$\mathcal{E}^*(u, M) \leq Q_a (\max_{T \in M} C'_T) \|e\|_E$$

where

$$Q_a = C_a C'_a = \max_{T \in M} \frac{a|_T}{a|_{T'}}$$

and we get (4.3).

6 The Experimental Results

In this section we will experimentally verify the reliability of various conclusions that can be made from Theorems 4.1, 4.2 for the given estimator.

6.1 The Influence of Mesh Topology

Theorem 4.1 was proven for general meshes without any restrictions on the mesh topology. Hence, it can be expected that particular meshes with different topologies could influence the effectivity index in the same order of magnitude as indicated by the theoretical upper and lower bounds. In addition the influence of the angle has to be visible (and could also depend on the topology). To check the validity of this conclusion for a smooth solution we consider the following problem:

For $\Omega = (0,1) \times (0,1)$, let u be the solution of

$$-\Delta u = f \text{ in } \Omega, \quad u = 0 \text{ on } \Gamma \tag{6.1}$$

We choose f such that $u = \sin \pi x \sin \pi y$.

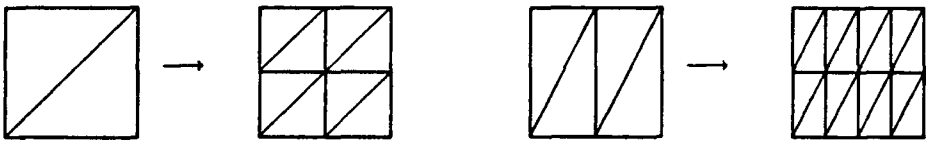

mesh ratio 1/1 mesh ratio 1/2

Figure 6.1: Regular three-direction mesh

6.1.1 Three-direction meshes

Let us consider the three-directional meshes which are obtained by uniform refinement of a basic mesh of the type $\frac{1}{n}, n = 1, 2, 4, 8$ as shown in Fig. 6.1.

In Table 6.1 we report the effectivity index for these meshes. We also report the upper and lower bounds for the effectivity index from Theorems 4.1, 4.2, when $p = 2$ was used.

number of	mesh			
elements	1/1	1/2	1/4	1/8
8	0.852			
16		0.993		
32	1.070		1.289	
64		1.183		1.804
128	1.147		1.503	
256		1.252		2.068
512	1.180		1.571	
1024		1.277		2.145
2048	1.192		1.594	
4096		1.287		2.169
upper bound	2.34	2.87	3.87	5.38
lower bound	0.29	0.21	0.15	0.12

Table 6.1: Effectivity index for problem 6.1 ($u = \sin \pi x \sin \pi y$) and 3-direction meshes

6.1.2 Criss-cross meshes

Let us consider now the 'criss-cross' meshes as shown in Fig. 6.2. The effectivity indices for these meshes are given in Table 6.2.

6.1.3 Diamond-shaped meshes

Finally, we consider the 'diamond-shaped' meshes as shown in Fig. 6.3. The effectivity indices are given in Table 6.3.

Comparing the tables we can make the following conclusions, which are in agreement with Theorems 4.1, 4.2:

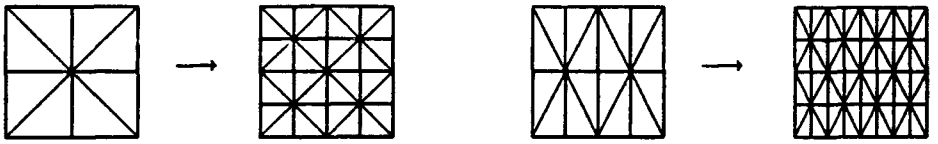

mesh ratio 1/1 mesh ratio 1/2

Figure 6.2: Regular criss-cross mesh

number of elements	mesh 1/1	1/2	1/4	1/8
8	1.350			
16		0.939		
32	1.036		1.049	
64		1.053		1.349
128	1.077		1.179	
256		1.085		1.518
512	1.088		1.214	
1024		1.093		1.562
2048	1.090		1.223	
4096		1.095		1.574
upper bound	2.34	2.87	3.87	5.38
lower bound	0.29	0.21	0.15	0.12

Table 6.2: Effectivity index for problem 6.1 ($u = \sin \pi x \sin \pi y$) and 'criss-cross' meshes

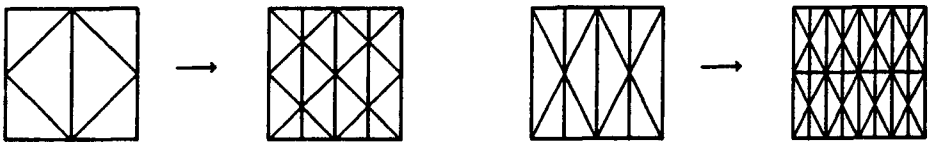

mesh ratio 1/1 mesh ratio 1/2

Figure 6.3: Regular 'diamond-shaped' mesh

number of elements	mesh 1/1	1/2	1/4	1/8
6	1.465			
12		0.750		
20	1.017			
24			0.523	
40		1.026		
48				0.385
72	1.107			
80			1.111	
144		1.188		
160				0.959
272	1.131			
288			1.558	
544		1.234		
576				1.708
1056	1.138			
1088			1.740	
2112		1.246		
2176				2.274
4160	1.139			
4224			1.793	
8448				2.515
upper bound	2.34	2.87	3.87	5.38
lower bound	0.29	0.21	0.15	0.12

Table 6.3: Effectivity index for problem 6.1 ($u = \sin \pi x \sin \pi y$) and 'diamond-shaped' meshes

1. For $h \to 0$ the effectivity index stays in the theoretical bounds. In addition we see that in our concrete case the effectivity index converges to a limiting value. This is not surprising, because the mesh is translation invariant and the solution can be periodically extended. In this case various results about superconvergence can be used (see [21]).
2. The effectivity index depends on the topology. The error estimator is not asymptotically exact.
3. The dependence of the effectivity index on the angle is clearly visible.
4. The theoretical bounds for the effectivity index are relatively pessimistic. This is because these bounds are independent of the topology and the solution. Better bounds in our case could be obtained by exploiting the superconvergence effect (see [5]).

6.2 The Influence of the Solution Structure

Theorems 4.1 and 4.2 have been shown for a general solution. We expect that the effectivity index may depend on the solution structure. To check this conclusion consider the solution of the following problem on $\Omega = (0,1) \times (0,1)$:

$$-\Delta u = f \text{ in } \Omega, \quad u = 0 \text{ for } x = 0 \text{ and } x = 1, \quad \frac{\partial u}{\partial y} = 0 \text{ for } y = 0 \text{ and } y = 1 \qquad (6.2)$$

with f such that $u = \sin \pi x$. We will use meshes as in Fig. 6.1 with the orientation shown there (mesh 1/2 and 1/4) and with the opposite orientation (2/1 and 4/1).

number of elements	mesh 1/1	1/2	1/4	2/1	4/1
8	1.013				
16		1.564		0.717	
32	1.107		2.258		0.507
64		1.598		0.783	
128	1.131		2.273		0.553
256		1.608		0.800	
512	1.137		2.278		0.566
1024		1.611		0.804	
2048	1.139		2.279		0.569
4096		1.612		0.806	
upper bound	2.34	2.87	3.87	2.87	3.87
lower bound	0.29	0.21	0.15	0.21	0.15

Table 6.4: Effectivity index for problem 6.2 ($u = \sin \pi x$) and 3-direction meshes

From Table 6.4 we see in fact that the effectivity index depends on the relation between the mesh and the structure of the solution (especially the relation between the second derivatives and the mesh orientation). Hence in general we have to deal with uncertainties in the effectivity index. (No correction factor could improve the situation.) We note that our factor $\kappa = 0.2684\ldots$ could be changed, but in general (for all functions) the range in the effectivity index could not be improved. Again, we see that Theorems 4.1 and 4.2 reliably predict the outcome of the numerical experiments.

6.3 The Influence of the Smoothness of the Solution

Theorems 4.1 and 4.2 contain higher order terms which we neglected in the reported theoretical bounds in Tables 6.1-6.4. when computing the bounds. These terms influence the convergence of the effectivity index as $h \to 0$. To check the effect of these terms we will consider once more problem 6.1, using now the solution

$$u(x,y) = \sin a\pi x \sin a\pi y. \tag{6.3}$$

(We use regular three-direction meshes, as in Fig. 6.1 with mesh ratio 1/1).

number of elements	$a=1$	$a=2$	$a=4$	$a=11$
8	0.852	0.833	0.438	
32	1.070	0.876	0.932	0.379
128	1.147	1.080	0.887	0.530
512	1.180	1.161	1.090	0.780
2048	1.192	1.187	1.168	1.022
8192				1.148
upper bound	2.34	2.34	2.34	2.34
lower bound	0.29	0.29	0.29	0.29

Table 6.5: Effectivity index for problem 6.3 ($u = \sin a\pi x \sin a\pi y$) and 3-direction meshes

We see that the insufficient smoothness influences the effectivity index and that the effectivity index can behave erratically. Nevertheless the bounds —where higher order terms are neglected— are still valid. We see in general that the effectivity index decreases with decreasing smoothness of the solution. The lower bound goes down with increasing p, but the upper bound is not influenced. Hence we can expect that the effectivity index will go down (assuming heuristically that the effecitivity index moves as the middle of the interval). The same effect will be seen later. Once more we see good agreement with the conclusions stemming from Theorem 4.1 and that we cannot hope for the existence of a universal correction factor.

6.4 Harmonic solutions

The error estimator contains terms related to the residual and the jumps, respectively. To isolate the influence of the jump term, we consider the following problem (again in $\Omega = (0,1) \times (0,1)$):

$$-\Delta u = 0 \text{ in } \Omega, \quad u = 0 \text{ for } x = 0, x = 1 \text{ and } y = 0, \quad \frac{\partial u}{\partial n} = g \text{ for } y = 1 \tag{6.4}$$

and let $u(x,y) = \sin \pi x \sinh \pi y$. The effectivity index (for a regular three-direction mesh as shown in Fig. 6.1) is given in Table 6.6.

Comparing Table 6.1 and 6.6 we see a similar behaviour influenced only mildly by the structure of the solution. The limiting value for the effectivity index seems to be different for the mesh 1/1. For the other meshes this effect is less visible. For these particular meshes, this might be explained by a superconvergence phenomenon.

number of elements	mesh 1/1	1/2	1/4	1/8
8	0.841			
16		0.958		
32	0.978		1.269	
64		1.102		1.795
128	1.040		1.457	
256		1.166		2.042
512	1.065		1.534	
1024		1.190		2.136
2048	1.071		1.560	
4096		1.199		2.166
upper bound	2.34	2.87	3.87	5.38
lower bound	0.29	0.21	0.15	0.12

Table 6.6: Effectivity index for problem 6.4 ($u(x,y) = \sin \pi x \sinh \pi y$) and 3-direction meshes

6.5 Adaptively Constructed Meshes

So far, we have restricted our experiments to uniform meshes. We will now consider nonuniform meshes either based on an adaptive procedure or randomly refined. We use problem 6.4 again. We have constructed three sequences (A - C) of meshes. Each sequence is obtained by refining a part of the elements of the previous mesh according to a refinement indicator and adjusting neighbouring elements. In sequences A and B the refinement indicator was an error estimator (with different parameters), in sequence C the indicator was a random number. Typical meshes of each sequences are shown in Fig. 6.4. The effectivity indices are given in Table 6.7.

Sequence A		Sequence B		Sequence C	
elements	effectivity index	elements	effectivity index	elements	effectivity index
8	0.841	8	0.841	8	0.841
19	0.944	19	0.944	23	0.906
47	0.970	38	0.941	45	0.964
94	1.008	67	0.980	96	1.008
181	1.018	107	0.949	200	0.979
323	1.041	201	1.013	435	0.990
593	1.043	355	1.039	964	0.972
1020	1.060	607	1.032	2129	1.008
1773	1.051	991	1.056	4588	0.992

Table 6.7: Effectivity indices for problem 6.4 and nonuniform meshes

Comparing Tables 6.7 and 6.6 we see that different refinement strategies lead to different effectivity indices, although the difference is not big. Once more we see a range of the effectivity indices. We note that for these general meshes superconvergence results cannot be applied.

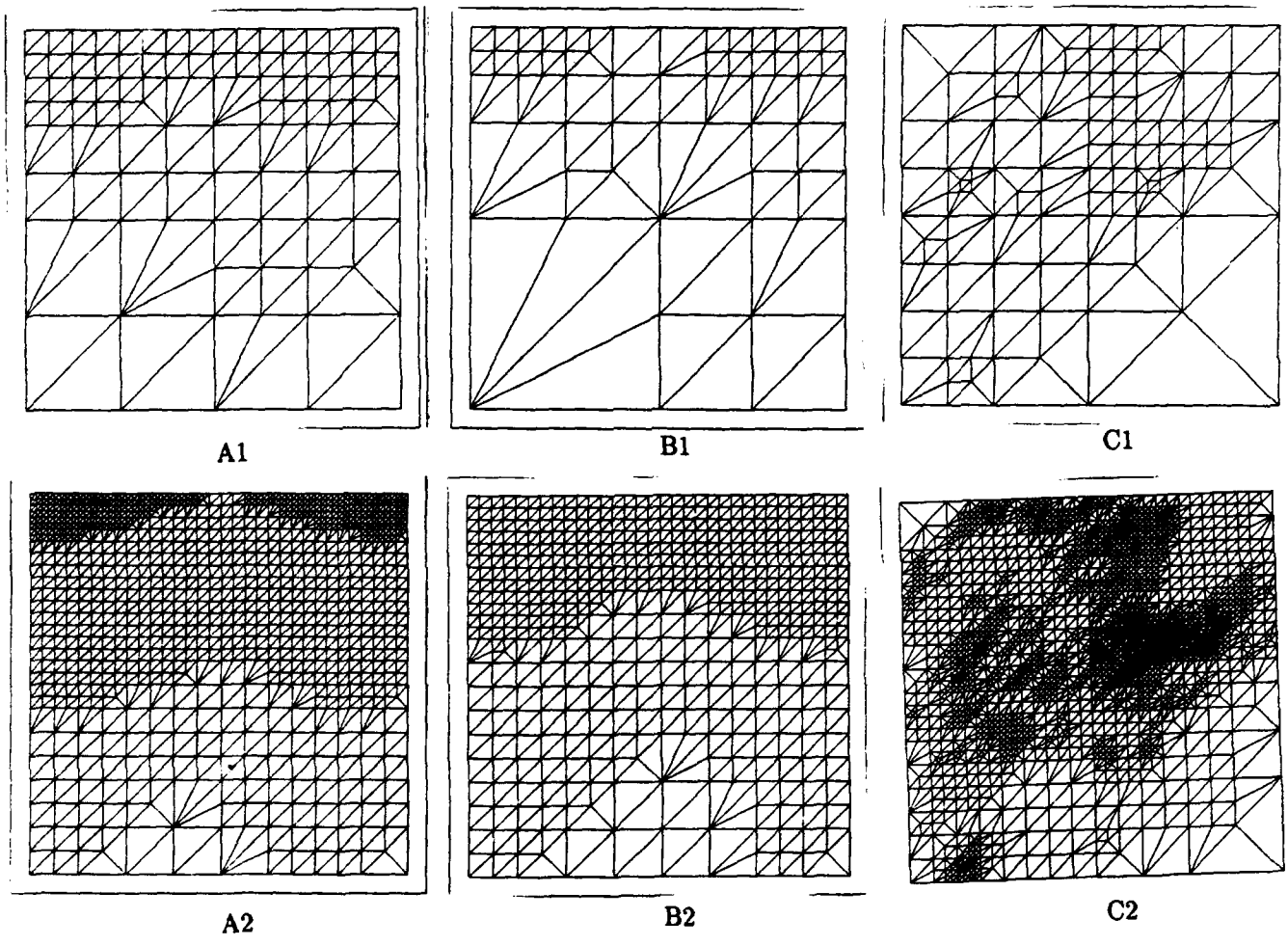

Figure 6.4: Nonuniform meshes for problem 6.4

6.6 Effectivity Indices for Problems with Unsmooth Solutions

So far, we have considered problems with a smooth solution. Let us now examine the behaviour of the error estimator for solutions with singularities. Theorems 4.1 and 4.2 indicate a decrease of the effectivity index, when the singularity of the exact solution grows, and also that this effect diminishes when adaptive meshes are used.

To this purpose we consider the domain $\Omega = (-1,1) \times (-1,1)$, partitioned into 4 square subdomains as shown in Fig. 6.5. Let u be the solution of

$$-\nabla(a(x,y)\nabla u) = 0 \text{ in } \Omega, \quad a(x,y)\frac{\partial u}{\partial n} = g(x,y) \text{ on } \Gamma \tag{6.5}$$

where $a(x,y)$ is constant in each quadrant ($a(x,y) = 1$ or $a(x,y) = \tilde{a}$, see Fig. 6.5). $\tilde{a}$ is chosen so that

$$u(x,y) = r^{\alpha}(c_i \cos(\alpha\varphi) + s_i \sin(\alpha\varphi)) \tag{6.6}$$

where (r,φ) are polar coordinates with center in the origin. For $\alpha = 0.5$ and $\alpha = 0.1$ we get $\tilde{a} = 3 + \sqrt{8} \approx 5.828\ldots$ and $\tilde{a} \approx 166.447\ldots$, respectively.

2 $a(x,y) = \tilde{a}$	1 $a(x,y) = 1$
3 $a(x,y) = 1$	4 $a(x,y) = \tilde{a}$

Figure 6.5: Coefficient a for problem 6.5

Table 6.8 shows the effectivity index for uniform meshes. (In each quadrant the meshes are uniform three-direction meshes of mesh ratio 1/1 as in Fig. 6.1. The orientation of the meshes is changed in subdomains 2 and 4 to preserve the symmetry of the solution.)

number of		
elements	$\alpha = 0.5$	$\alpha = 0.1$
32	0.658	0.520
128	0.694	0.512
512	0.711	0.524
2048	0.719	0.536
8192	0.722	

Table 6.8: Effectivity index for problem 6.5 ($u = r^{\alpha} f(\varphi)$) and 3-direction meshes

Although the estimator in Theorem 4.1 includes the ratio of a, it influences only elements on the interfaces and hence this factor can be neglected. The decrease of the effectivity index is clearly related to the necessity to use a higher degree p in 4.2 for the estimate. Hence the

unsmoothness of the solution decreases the effectivity index. This has also been observed in Table 6.5.

We have seen in Table 6.7, that nonuniformity of the mesh does not influence the effectivity index too much. On the other hand an adaptive procedure refines the mesh in the places where the solution in unsmooth and hence a lower p can be used. We have created two sequences of adaptively refined meshes (A and B). The meshes B1 and B2 are less refined than the meshes A1 and A2. The refinement in meshes B is more concentrated around the origin than in meshes A. Examples of each sequences are displayed in Fig. 6.6. If the mesh is properly refined , a lower p can be used and the effectivity index improves. Table 6.9 confirms this conclusion (for $\alpha = 0.5$).

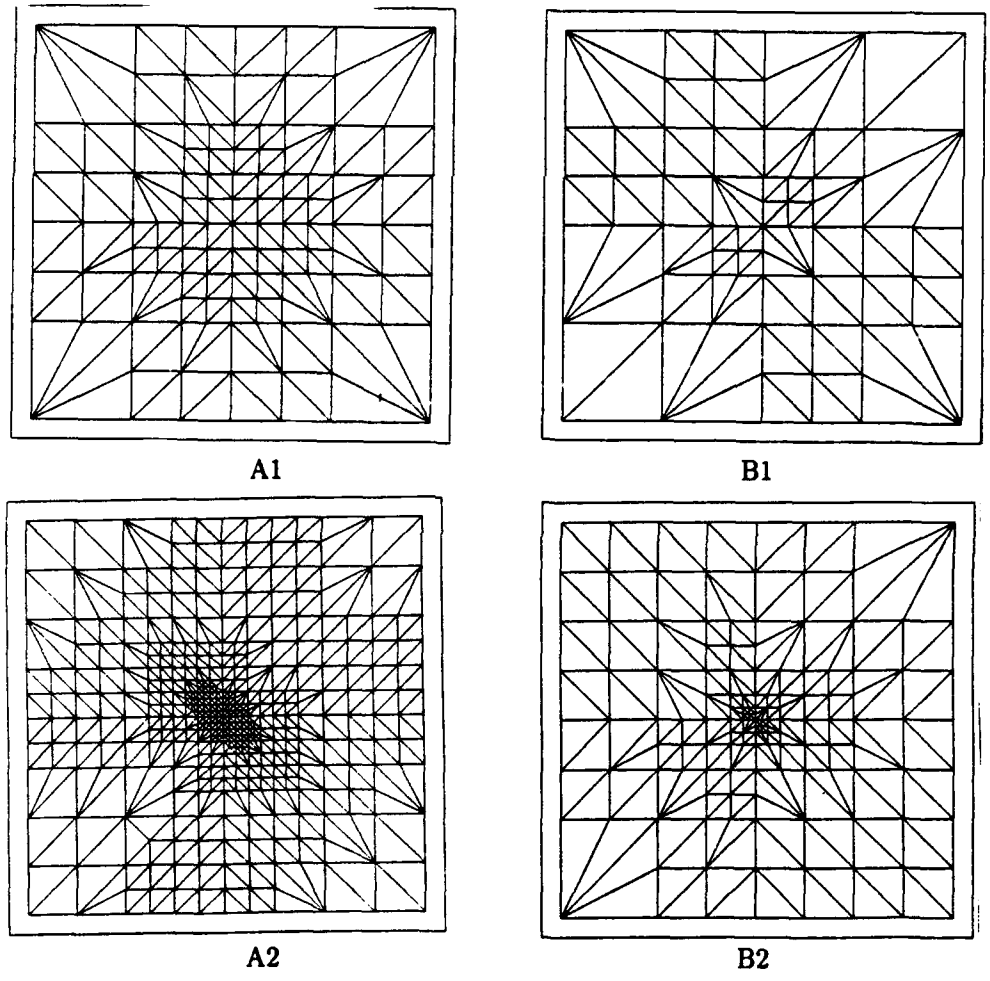

Figure 6.6: Nonuniform meshes for problem 6.5

The effect of the unsmoothness of the solution can also be observed if the singular part of the solution is removed. So we consider problem 6.5 in the domain $\tilde{\Omega} = \Omega - [-0.5, 0.5] \times [-0.5, 0.5]$ and prescribe $a\frac{\partial u}{\partial n} = g$ on $\partial\tilde{\Omega}$. Table 6.10 shows the effectivity indices for this problem using uniform meshes as for Table 6.8. Again, $\alpha = 0.5$.

We note that the effectivity index is now very similar to problems 6.1, 6.2.

Sequence A		Sequence B	
elements	effectivity index	elements	effectivity index
32	0.658	32	0.658
87	0.712	64	0.719
194	0.738	96	0.787
370	0.761	168	0.830
725	0.787	244	0.880
1297	0.807	363	0.918
2346	0.828	485	0.960
		604	0.959
		768	0.975
		965	0.995

Table 6.9: Effectivity indices for problem 6.5 ($u = r^\alpha f(\varphi)$) and adapted meshes

number of elements	$\alpha = 0.5$
24	0.964
96	1.027
384	1.059
1536	1.070
6144	1.073

Table 6.10: Effectivity index for problem 6.5 ($u = r^\alpha f(\varphi)$ on $\tilde{\Omega}$) and 3-direction meshes

6.7 The Oscillation Effect

It is often assumed, that the error of the interpolant is close to the error of the finite element method. To demonstrate that this assumption is in general incorrect, we show that the error of the finite element method could oscillate. To this end we show in Fig. 6.7 the typical error behaviour for the problem discussed in section 6.6 with uniform meshes and $\alpha = 0.5$. Displayed are two patches of regular three-direction meshes at the same location—far from the singularity—in Ω. Fig. 6.7 also shows the error indicators (in parentheses). In Fig. 6.8 we illustrate graphically the error behaviour for the entire mesh where the mesh has 363 elements. (An element is black if the energy norm error in this element exceeds a certain threshold. Here, the threshold is 4.0×10^{-4}.)

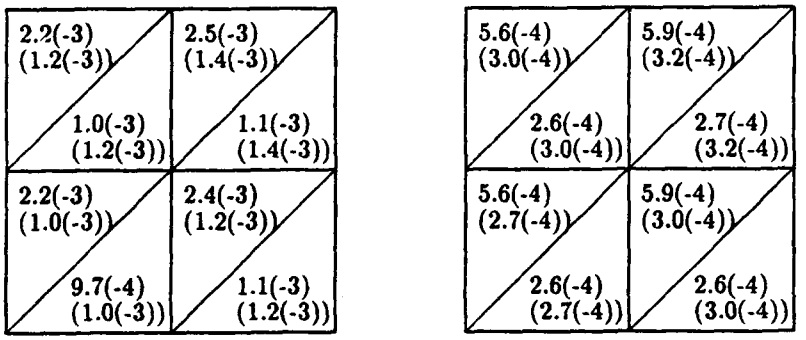

small element side: 1/8 small element side: 1/16

values in (..): error estimator

Figure 6.7: Oscillation of the finite element error

We see that the error indicator shows approximately the average error for adjacent elements and hence does not exhibit the oscillation of the error of the finite element solution. Note that the interpolant does not show the oscillation. This oscillation effect is caused by the pollution of the error stemming from the singularity of strength $r^{1/2}$. If we enforce a smooth solution by removing the center part of the domain, as in problem 6.5, the results given in Fig. 6.9 show that the oscillation disappears. (We use elements from the same location as in Fig. 6.7; the numbers are therefore directly comparable.)

The oscillation effect is weaker, if $\alpha \neq 0.5$ or the mesh is constructed adaptively. We show in Fig. 6.10 the local results for $\alpha = .8$ and in Fig. 6.11 the results for $\alpha = .5$ and adaptively refined meshes. In Fig. 6.12 we show the error behaviour for an adaptively refined mesh and the threshold 2.0×10^{-3}. In Section 7 we will examine this effect.

7 Analysis of the Oscillation Phenomenon

The oscillation phenomenon we have observed in Section 6.7 occurs also in the case of the following problem on $\Omega = [-1, 1] \times [0, 1]$

$$-\Delta u = 0 \text{ in } \Omega, \quad u = 0 \text{ on } \Gamma_D = \{(x, y) \mid 0 \leq x \leq 1, y = 0\}, \quad \frac{\partial u}{\partial \mathbf{n}} = g \text{ on } \Gamma_N = \Gamma - \Gamma_D$$

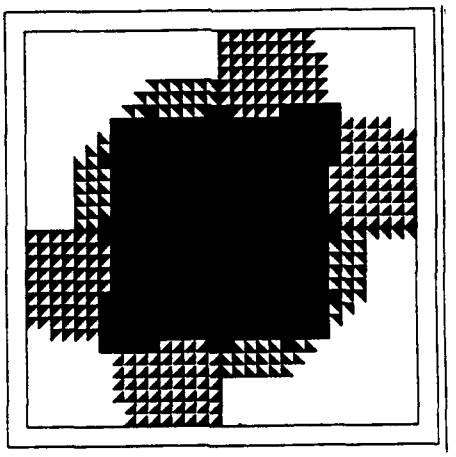

Figure 6.8: Finite element error ($\alpha = 0.5$, uniform meshes)

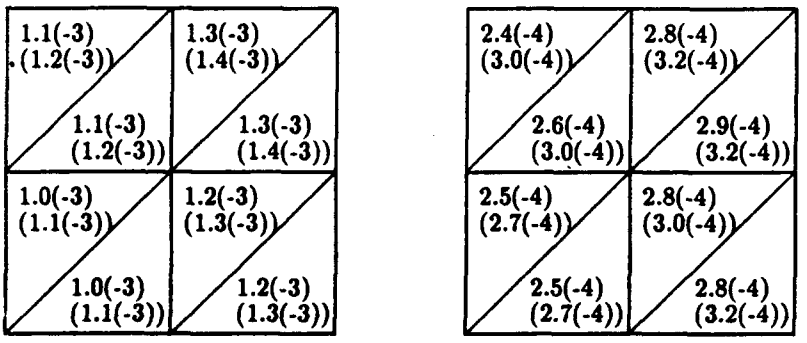

small element side: 1/8 small element side: 1/16

values in (..): error estimator

Figure 6.9: Finite element error and estimators for a problem without singularity

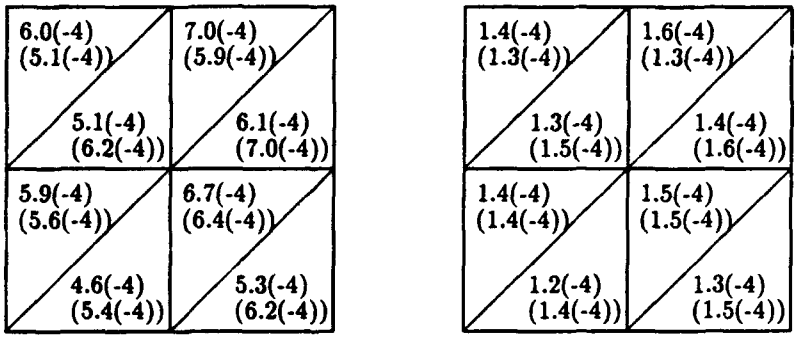

small element side: 1/8 small element side: 1/16

values in (..): error estimator

Figure 6.10: Finite element error and estimators for problem with singularity ($\alpha = .8$, uniform mesh)

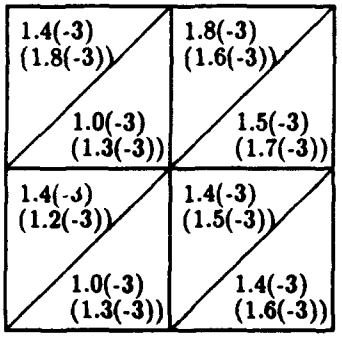

small element side: 1/8

values in (..): error estimator

Figure 6.11: Finite element error and estimators for problem with singularity ($\alpha = .5$, adaptively refined mesh)

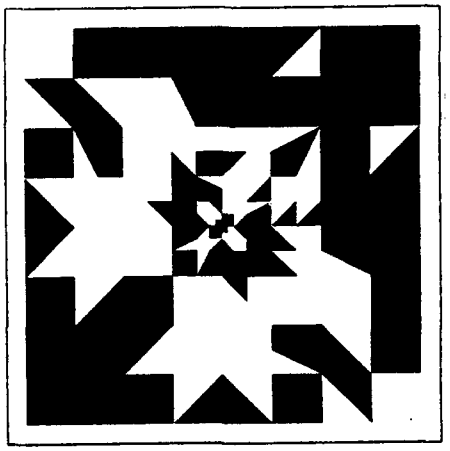

Figure 6.12: Finite element error for adapted mesh ($\alpha = 0.5$)

with g selected so that

$$u = r^{1/2}\sin(\frac{1}{2}\varphi) = \mathrm{Re}z^{1/2}$$

with $z = x + iy$.

We consider now a uniform 3-direction mesh of the type shown in Fig. 6.1. Then the finite element solution has essentially the form

$$u_S(x,y) = u^I(x,y) + G(x,y) + R(x,y), \tag{7.1}$$

where $\|R(.,.)\|_{H^1} \leq o(h)$ and $G(x,y)$ is a piecewise linear function, which coincides in the nodal points of the mesh with the function

$$G^*(x,y) = Ar^{-1/2}\sin\frac{1}{2}\theta h = Ah\mathrm{Re}z^{-1/2}. \tag{7.2}$$

The function $G^*(x,y)$ is the adjoint singularity function. It describes the pollution error, which is of the same order (in $\|.\|_E$) as the error of the interpolant. The error—measured in the energy norm—is locally (i.e. on single elements) of order h^2 and is governed by the second derivatives of u. The contributions of G to the energy error are of the same order, but are governed by the first derivative of G. Now observe that in our case both errors are governed by the second derivative of $\mathrm{Re}z^{1/2}$. This leads to a cancellation and consequently to the oscillation phenomenon.

To demonstrate this, we consider a patch of two triangles as in Fig. 7.1 with local coordinates ξ, η with the origin in the lower left vertex of the patch.

Using (7.1), (7.2) we can assume that on the patch:

$$\begin{aligned} u &= a(\xi^2 - \eta^2) + b\xi\eta + \text{linear functions} + \text{h.o.t.} \\ G &= (\alpha a\xi + \alpha b\eta)h + \text{constant term} + \text{h.o.t.} \end{aligned}$$

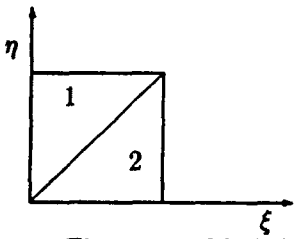

Figure 7.1: Mesh for local analysis of errors

where α is related to A in (7.2). Neglecting R in 7.1, we get by simple computations

$$\frac{\|e\|_{E1}^2}{\|e\|_{E2}^2} = \frac{(a^2+b^2)(1+2\alpha+3\alpha^2)+a^2}{(a^2+b^2)(1-2\alpha+3\alpha^2)+a^2}$$

($\|e\|_{E_i}$ is the energy norm of the error in element i) and we see that we have in the case without pollution ($\alpha = 0$)

$$\frac{\|e\|_{E1}^2}{\|e\|_{E2}^2} = 1$$

while the ratio is $\neq 1$ in the presence of the pollution error. This explains our observation in Section 6.7.

Let us note that the said effect occurs when the pollution error and the error of the interpolant have the same strength. This is in agreement with our results in Section 6.7, where the oscillation phenomenon was only visible for the singularity $\alpha = .5$.

8 Conclusions

Summarizing the results that we have presented in the previous sections we draw the following conclusions.

1. The estimator performs as expected from its properties given in Theorems 4.1 and 4.2.
2. The effectivity index depends on the mesh, especially on the angle of the triangles. Hence meshes without small angles are preferable. The notion of the angle depends on the differential operator.
3. The effectivity index is not too sensitive to the topology of the mesh (except for the minimal angle).
4. The effectivity index can be larger or smaller than 1 depending on the character of the solution as predicted in Theorems 4.1 and 4.2.
5. If the solution has singular behaviour, the quality of the error estimator deteriorates. The deterioration can be avoided by adaptive refinement, as follows from Theorem 4.1.

References

[1] I. Babuška, R. Durán, and R. Rodríguez. Analysis of the efficiency of an a-posteriori error estimator for linear triangular elements. to be published in SIAM J. Numer. Anal.

[2] I. Babuška and W. C. Rheinboldt. Error estimates for adaptive finite element computations. *SIAM J. Numer. Anal.*, 15:736–755, 1978.

[3] I. Babuška and W. C. Rheinboldt. A posteriori error estimates for the finite element method. *Internat. J. Numer. Meths. Engrg.*, 12:1597–1615, 1978.

[4] I. Babuška and W. C. Rheinboldt. Reliable error estimation and mesh adaptation for the finite element method. In J. T. Oden, editor, *Computational Methods in Nonlinear Mechanics*. North-Holland Publishing Company, 1978.

[5] I. Babuška and R. Rodríguez. The problem of the selection of an a-posteriori error indicator based on smoothing techniques. Technical Report BN 1126, University of Maryland at College Park, Inst. for Phys. Sc. and Techn., 1991.

[6] I. Babuška and M. Suri. The h-p version of the finite element method with quasiuniform meshes. *Model Math. Anal. Numer. (RAIRO)*, 21:199–238, 1987.

[7] I. Babuška and D. Yu. Asymptotically exact a-posteriori error estimator for biquadratic elements. In *Finite Elements in Analysis and Design 3*, 1987.

[8] I. Babuška, O. C. Zienkiewicz, J. Gago, and E. R. de A. Oliveira, editors. *Accuracy Estimates and Adaptive Refinements in Finite Element Computations*. John Wiley & Sons, Chichester, 1986.

[9] P. L. Baehmann, M. S. Shephard, and J. E. Flaherty. A-posteriori error estimation for triangular and tetrahedral quadratic elements using interior residuals. Technical Report SCOREC Rep 14-1990, Rensselaer Polytechnic Institute, Troy, New York, 1990.

[10] R. E. Bank and B. D. Welfert. A-posteriori error estimates for the Stokes equation: A comparison. *Comput. Meths. Appl. Mech. Engrg.*, 82:323–340, 1990.

[11] R. Duran, M. A. Muschietti, and R. Rodríguez. On the asymptotic exactness of error estimators for triangular finite elements. *Numer. Math.*, 59:107–127, 1991.

[12] R. E. Ewing. A-posteriori error estimation. *Comput. Meths. Appl. Mech. Engrg.*, 82:59–72, 1990.

[13] J. T. Oden. Adaptive finite element methods for problems in solid and fluid mechanics. In D. L. Dwoyer, M. Y. Hussaini, and R. G. Voigt, editors, *Finite Elements, Theory and Applications*. Springer Verlag, New York, 1988.

[14] J. T. Oden, L. Demkowitz, L. Rachowitz, and T. A. Westermann. Towards a universal h-p adaptive finite element strategy. part 2: A-posteriori error estimation. *Comput. Meths. Appl. Mech. Engrg.*, 77:113–180, 1989.

[15] J. T. Oden, L. Demkowitz, L. Rachowitz, and T. A. Westermann. A-posteriori error analysis in finite elements: The residual method for symmetrizable problems with applications to compressible Euler and Navier-Stokes equations. *Comput. Meths. Appl. Mech. Engrg.*, 82:183–204, 1990.

[16] L. Plank, E. Stein, and D. Bischoff. Accuracy and adaptivity in the numerical analysis of thin-walled structures. *Comput. Meths. Appl. Mech. Engrg.*, 82:223–256, 1990.

[17] M. S. Shephard, Q. Niu, and P. L. Baehmann. Some results using projectors for error indication and estimation. In J. E. Flaherty, P. J. Paslow, M. S. Shephard, and J. D. Vasilakis, editors, *Adaptive Methods in Partial Differential Equations*, pages 83–99. SIAM Philadelphia, 1989.

[18] T. Strouboulis and K. A. Haque. Recent experiences with error estimation and adaptivity. Part I. Review of error estimators for scalar elliptic equations. submitted to Comp. Meth. Appl. Mech. Eng., 1991.

[19] T. Strouboulis and K. A. Haque. Recent experiences with error estimation and adaptivity. Part II. Error estimation for h-adaptive approximations on grids of triangles and quadrilaterals. submitted to Comp. Meth. Appl. Mech. Eng., 1991.

[20] R. Verfürth. A-posteriori error estimators for the Stokes equation. *Numer. Math.*, 55:309–325, 1989.

[21] L. B. Wahlbin. Local behaviour in finite element methods. In P. G. Ciarlet and J. L. Lions, editors, *Handbook of Numerical Analysis*, volume 2, pages 353–522. North Holland, 1991.

[22] J. Z. Zhu and O. C. Zienkiewicz. Adaptive techniques in the finite element method. *Comm. Appl. Num. Meth.*, 4:197–204, 1988.

[23] O. C. Zienkiewicz and J. Z. Zhu. A simple error estimator and adaptive procedure for practical engineering analysis. *Internat. J. Numer. Meths. Engrg.*, 24:337–357, 1987.

[24] O. C. Zienkiewicz and J. Z. Zhu. The three R's of engineering analysis and error estimation and adaptivity. *Comput. Meths. Appl. Mech. Engrg.*, 82:95–114, 1990.

The **Laboratory for Numerical Analysis** is an integral part of the Institute for Physical Science and Technology of the University of Maryland, under the general administration of the Director, Institute for Physical Science and Technology. It has the following goals:

- To conduct research in the mathematical theory and computational implementation of numerical analysis and related topics, with emphasis on the numerical treatment of linear and nonlinear differential equations and problems in linear and nonlinear algebra.

- To help bridge gaps between computational directions in engineering, physics, etc., and those in the mathematical community.

- To provide a limited consulting service in all areas of numerical mathematics to the University as a whole, and also to government agencies and industries in the State of Maryland and the Washington Metropolitan area.

- To assist with the education of numerical analysts, especially at the postdoctoral level, in conjunction with the Interdisciplinary Applied Mathematics Program and the programs of the Mathematics and Computer Science Departments. This includes active collaboration with government agencies such as the National Institute of Standards and Technology.

- To be an international center of study and research for foreign students in numerical mathematics who are supported by foreign governments or exchange agencies (Fulbright, etc.).

Further information may be obtained from **Professor I. Babuška**,Chairman, Laboratory for Numerical Analysis, Institute for Physical Science and Technology, University of Maryland, College Park, Maryland 20742-2431.